8. Source Contribution Assessment Methodology

This section addresses the methodology that was used to estimate the contribution of the Mohave Power Project to ambient sulfate concentrations and light extinction at Grand Canyon National Park. Because of the topographic and meteorological complexity of the study environment, no single attribution model was expected to be usable under all circumstances. Rather, the overall attribution approach consisted of the use of several techniques in concert to strive to obtain a credible range of attribution estimates.

An initial effort at estimating attribution used several receptor analysis techniques and simulation models, which were applied without knowledge of the results of the perfluorocarbon tracer (PFT) experiments that took place during the two intensive study periods. The modeling results were then tested against the measured PFT concentrations and it was found that the models generally performed poorly, as we describe below in Section 8.2. To provide improved predictions, the information from the PFT experiments was incorporated into new or revised models, either as input or as a basis for setting parameters. The approaches that resulted, described in Section 8.3, were then used to develop the final attribution estimates of the study, as presented in Section 9.

8.1 Overview of Attribution Approach

The process of identifying and quantifying the estimated impact of MPP's emissions on Grand Canyon sulfate concentrations and light extinction was accomplished using two types of assessment tools.

The first type – receptor data analysis or receptor modeling – is an analysis of concentration and chemical composition data collected at one or more receptor locations, sometimes in combination with meteorological information, and comparison of the receptor data with the composition of emissions from sources of interest. Receptor modeling is a diagnostic approach that analyzes measurements to derive a plausible accounting of the emissions that produced measured concentrations and compositions. Although conceptually straightforward, receptor modeling depends on accurate measurements of ambient concentrations and, in many cases, on accurate characterization of the compositions of emissions from major source categories. In practice, some receptor analysis methods can be statistically complex. Receptor analysis can only be used to analyze conditions at the times and locations for which measurements exist; it has no predictive capability for other times and locations.

The fundamental assumption for many of the receptor-oriented methods is that the concentration of the tracer is in the same ratio to the concentration of the species of interest (e.g., total sulfur from the MPP) at both the source and receptor. This means that the tracer emissions are assumed to accurately follow the SO_2 emissions rate from the MPP stack and that the tracer and the target species all undergo diffusion, deposition, and conversion at the same rates. In practice this limits such methods to inert gaseous or fine particle species with minimal deposition. Hybrid models, that add a parametric representation of chemical conversion and/or deposition to the basic receptor model, are used to overcome this limitation. Several of the receptor models used for Project MOHAVE are of this hybrid form.

The second method – source emissions simulations or simulation modeling –uses mathematical models of the transport, diffusion, deposition, and chemical conversion of the emitted air pollutants to predict ambient concentrations resulting from emissions. Such models, which rely on our understanding of the physics and chemistry of the atmosphere, are conceptually able to predict air quality impacts at all locations and times. Because of limitations in our knowledge of atmospheric behavior, our ability to portray that knowledge mathematically, and the ability of computers to carry out the needed calculations in a reasonable amount of time, all models require some input data on meteorology and air quality, in addition to the obvious requirement of emissions information.

It needs to be recognized that it is an extremely difficult task to predict with reasonable accuracy the tracer concentrations at Meadview and Hopi Point which are located approximately 110 km and 280 km away from the MPP point source, respectively. Rugged terrain, lakes and rivers exist between the source and receptors. In this setting, the atmospheric system is complex, and therefore models that attempt to portray its behavior faithfully tend to be complex and are very sensitive to small errors in assumptions about processes. Models that use more measured information or simplify the mathematical representations of processes tend to be simpler, but, in turn, may suffer from errors due to that simplification. Furthermore, as was noted in Section 1.1, the outage study concluded that the average MPP contribution to sulfate at Meadview was less than 15%. Therefore, it was essential that the reasonableness or accuracy of simulation modeling be tested against measurements, as they were in Project MOHAVE.

The concentrations that are calculated at specific receptor points by emission simulation models are very sensitive to the input wind field description, particularly the wind direction. A small error in wind direction can change plume impact at a distant receptor from a “direct hit” to a complete miss, or vice versa. (For example, the straight-line distance from MPP to Meadview is 110 km, so a 5° difference in mean wind direction will shift the centerline of the MPP plume by 10 km in the crosswind direction.) Because a dense grid of wind field measurements was not available, interpolation of measurements in space and time was necessary to construct a complete wind field for modeling. Modelers used several different schemes to construct representations of complete wind fields.

8.2 Evaluation of Initial Attribution Methods

Initial efforts to determine the contribution of the Mohave Power Project to ambient air quality were unsuccessful. Four dispersion modeling techniques and two receptor modeling approaches were applied, using meteorological and air quality measurements made during the two Project MOHAVE intensive study periods. The predictions were tested against 12- and 24-hour measurements of concentrations of the perfluorocarbon tracer (PFT) that was released from the MPP at the same time. (The PFT data were not available to the modelers when they prepared their predictions.)

The models tested are listed below. (The references given here describe the models, not their application for this evaluation.)

- HAZEPUFF, a Lagrangian puff model (Latimer, 1993)

- DRI/CSU Lagrangian Particle Model. The Colorado State University Lagrangian particle dispersion model (Uliasz and Pielke, 1993), with wind fields from the Desert Research Institute three-dimensional second order closure mesocale meteorological model (Enger, *et al*; 1993; Enger and Koracin, 1994)

- DRI semi-Gaussian trajectory-type dispersion model (Enger, 1990), using the same wind fields as used for the DRI/CSU Lagrangian Particle Model

- VISHWA. Use of source-receptor transfer coefficients from VISHWA, an Eulerian grid-based regional air quality model that was applied by the Grand Canyon Visibility Transport Commission using meteorological fields produced by the RAMS meteorological model (Tombach *et al.*, 1996)

- NPS Chemical Mass Balance (CMB). A simplified chemical mass balance approach that apportioned secondary sulfate, applied by the National Park Service

- BYU CMB. An application of the CMB approach using regional source profiles, by Brigham Young University

- RMAPS. A spatial pattern correlation model (Henry, 1997a and 1997b).

Table 8-1 presents the results of the evaluations, from Green and Tombach (1998), for all methods but RMAPS. The PFT used for those evaluations was the ocPDCH (ortho-cis-perfluorodimethylcyclohexane) isomer portion of the oPDCH tracer injected into the MPP stack effluent. It was assumed for the purposes of this evaluation that the measured PFT concentrations were free of error. In reality, as shown in Section 4.4, the ocPDCH precision was about 6% of the mean measured concentration listed for Meadview in Table 8-1. That same precision represents about one-third of the Hopi Point average concentration, however, so some of the performance evaluations reflect measurement uncertainty. The accuracy of the PFT measurements has not been characterized.

None of these techniques was successful at predicting the ambient 12- and 24-hour average PFT concentrations reliably. The best correlation between the predicted and measured concentrations was $r^2 = 0.17$, for HAZEPUFF model predictions of 12-hour concentrations at Hopi Point (where the measurements are more uncertain); this means that the model was able to account for 17% of the variation in the ocPDCH observations at Hopi Point. The concentrations predicted by HAZEPUFF averaged more than twice those measured, however. Furthermore, the same model only achieved an insignificant r^2 of 0.02 for predictions at the Meadview receptor, where the observed concentrations were higher and more precise than at Hopi Point.

Values of r^2 for all other methods were less than 0.1, both for predictions at Hopi Point and Meadview. This performance was not acceptable for meeting the Project MOHAVE objectives, particularly since the ability to predict secondary sulfate concentrations can be expected to be even poorer than it was for predicting the inert PFT tracer concentrations.

In addition to the models described in Table 8-1, predictions by a spatial pattern correlation receptor model, RMAPS (Henry, 1997a) were also evaluated. RMAPS apportions the average

concentration of a species, as measured at many sites, among several spatially distinct sources and can be applied to primary or secondary species; no assumptions concerning transformation or deposition rates are required.

RMAPS has been applied to predict the impacts of emissions from several source regions, including a "Colorado Valley Source" located in the vicinity of MPP and the Las Vegas area (Henry, 1997b). Green and Tombach (1999) describe tests of the RMAPS concentration predictions for the Colorado Valley Source against the maximum particulate sulfur that could be attributed to MPP based on measured PFT concentrations and assuming 100% conversion of SO_2. This comparison was done at 21 receptor locations, with concentrations averaged over the summer intensive.

Table 8-1 Summary of Evaluations of Initial Attribution Methods against PFT Measurements

Model	Mean conc., fl/l	Standard deviation, fl/l	Coeff. of variation	Bias (pred./ meas.)	Correl. coeff., r	RMS error, fl/l	RMS error/ mean meas. conc.
Meadview, 12 hour averages							
Observed ocPDCH[1]	0.91	0.93	1.02				
DRI/CSU[1]	0.55	0.93	1.71	0.60	-0.04	1.39	1.53
HAZEPUFF[1]	1.88	1.60	0.85	2.07	0.14	1.99	2.18
NPS CMB[1]	3.64	1.57	0.43	3.98	0.18	3.20	3.50
Observed ocPDCH[2]	1.15	1.11	0.97				
BYU CMB[2]	0.15	0.14	0.94	0.13	0.11	1.51	1.32
Meadview, 24 hour averages							
Observed ocPDCH[3]	0.95	0.68	0.72				
DRI Semi-Gaussian[3]	0.77	1.40	1.81	0.81	0.00	1.56	1.65
Hopi Point, 12 hour averages							
Observed ocPDCH[4]	0.20	0.17	0.83				
VISHWA[4]	0.24	0.41	1.74	1.19	0.30	0.40	1.97
HAZEPUFF[4]	0.57	0.68	1.21	2.83	0.43	0.73	3.62
Observed ocPDCH[5]	0.24	0.16	0.69				
BYU CMB[5]	0.12	0.22	1.94	0.49	0.03	0.31	1.32

[1] For those 12-hour periods with DRI/CSU, HAZEPUFF, and NPS ocPDCH predictions at Meadview (n=81).
[2] For those 12-hour periods with BYU ocPDCH predictions at Meadview (n=41).
[3] For those 24-hour periods with DRI/semi-Gaussian ocPDCH predictions at Meadview (n=38).
[4] For those 12-hour periods with VISHWA and HAZEPUFF ocPDCH predictions at Hopi Point (n=99).
[5] For those 12-hour periods with BYU ocPDCH predictions at Hopi Point (n=53).

The RMAPS-predicted spatial patterns for emissions from the Colorado Valley Source showed significant impact south of MPP, while such impact was not observed in the tracer data.

Specifically, for 13 of these receptors, mostly located in the 180-degree sector to the south of MPP, the RMAPS predictions exceeded the maximum amount of particulate sulfur that could be created from MPP emissions. The excess was sometimes more than a factor of two and in all cases was well beyond the uncertainty bounds assigned to the RMAPS and PFT tracer calculations. Based on these observations, Green and Tombach (1999) concluded that the RMAPS predictions of the impacts of the Colorado Valley Source are not a valid representation of the impacts of MPP. The reasons for this discrepancy have not been analyzed.

8.3 Descriptions of Final Attribution Methods

Since the initial modeling approaches lacked skill in transporting emissions to the correct locations, it was decided to use the PFT information on the transport and diffusion of the MPP plume and of emissions from the other tracer sources to endeavor to produce more credible attributions of sulfate. As a result, all of the methods that were ultimately used to attribute air quality and light extinction impacts to the Mohave Power Project and other sources relied to some degree on the PFT measurements. These methods, which are described in this section and summarized in Table 8-2, provide the basis for the conclusions presented in Section 9. Full descriptions of their applications in Project MOHAVE are provided in the documents referenced in Table 8-2; copies of those documents that not generally available are included in Appendix C. Two of the methods (Modified CMB and Modified HAZEPUFF) are revisions of methods used in the initial evaluation (BYU CMB and HAZEPUFF, respectively).

It should be noted that those techniques that explicitly used the PFT information in their calculations are no longer general purpose models, but rather ones that have been "tailored" for Project MOHAVE and more specifically to the conditions during the tracer releases. These models cannot be assumed to have the same predictive ability in the absence of tracer data as they do when tracer data are available, especially when conditions differ from those that prevailed during the tracer releases. In that sense the source simulation models under these conditions are as limited in their forecast ability as are all receptor models.

Because of the limitations and uncertainties of the modeling methods, the results of any single method were not used in isolation to arrive at a source attribution. Rather, many different methods were used to reach consensus source attributions. As we describe below, mechanisms by which MPP and other sources could impact Grand Canyon National Park were conceptualized and then the modeling approaches were used to make the concepts more quantitative. The approaches used fall into two broad classes. Some of the approaches were quite rigorous but contained extreme assumptions, such as the assumption in the Tracer Max approach that 100% of MPP SO_2 is converted to sulfate, to make them tractable. Such approaches were useful for helping set the broad physical upper and lower bounds within which the actual attributions had to lie. Other approaches, that were typically theoretically more complex and used more realistic assumptions, were used to attempt to narrow the range within which the actual attribution might occur.

Brief descriptions of each method are provided below. Each technique has inherent in it some assumptions about atmospheric behavior. The key assumptions are discussed below and are summarized in Table 8-3.

Table 8-2 Methods Used to Estimate Source Contributions

Method	Description	Inputs	Outputs	Reference
RECEPTOR DATA ANALYSES				
Tracer Max (Tracer Scaling)	Estimation of total sulfur impacts by scaling PFT measurements; provides upper bound for potential sulfate impacts	PFT and particulate S concentrations at receptors; emission ratio of S/PFT;	Contribution of PFT source to ambient S; upper bound estimate of contribution to particulate S	Green and Tombach (1999)
Exploratory Data Analysis	Statistical analysis of SO_2, particulate sulfur, and PFT measurements	PFT, SO_2, and particulate sulfur concentrations and b_{sp} at receptors; meteorological classes	Spatial correlations of particulate sulfur, temporal correlations of PFT, SO_2, and particulate sulfur at specific sites	Mirabella and Farber (1999)
Tracer Regression	Regression of b_{ext} against PFT, industrial halocarbons, and water vapor mixing ratio	PFT, halocarbon, and mixing ratio measurements at receptors	Contributions to b_{ext} from emissions in source regions of the chosen tracers	White *et al.* (1999)
TAGIT	Estimation of sulfate impact by identifying unimpacted sites from PFT measurements	PFT and particulate S concentrations at multiple receptors	SO_2 and particulate S concentrations attributable to sources/source regions where PFT was emitted	Kuhns *et al.* (1999)
Modified CMB (MCMB)	Chemical mass balance receptor modeling, modified to account for conversion and deposition of SO_2 and sulfate	Source/source-regions and receptor concentrations of SO_2, sulfate, and markers -- elements, spherical aluminosilicate, b_{abs}; relative times of travel; ROME estimates of relative conversion rates for emissions from different sources/source-regions.	SO_x and sulfate attributable to sources/source- regions	Eatough, Farber and Watson (1999)
TMBR	Tracer mass balance regression; regressions of SO_2 against PFT and of particulate sulfur against PFT	Concentrations at receptors of PFT, SO_2, and particulate sulfur	SO_2 and particulate S concentrations attributable to MPP	Ames and Malm (1999)
DMBR	Differential mass balance regression; hybrid of tracer-based dilution calculation with parameterized deposition and conversion	Concentrations at receptors of PFT and SO_2; times of travel from source to receptors; estimates of conversion rates; index of cloud cover	SO_2 and particulate S concentrations attributable to MPP	Ames and Malm (1999)

Method	Description	Inputs	Outputs	Reference
SOURCE EMISSIONS SIMULATIONS				
Modified HAZEPUFF	Lagrangian puff model; interpolated wind field; first order sulfate chemistry	Wind profiler soundings, PFT and SO_2 emissions from MPP, relative humidity	Distribution of concentrations of PFT, $S0_2$, sulfate, and light scattering attributable to MPP	Latimer (1993); Mirabella (1996a; 1996b)
CALMET/ CALPUFF	Multi-layer Gaussian puff model with parameterized first order chemical conversion; diagnostic meteorological model	Surface and upper air meteorological data, topography, PFT and SO_2 emissions from MPP, solar radiation, ambient O_3	Distribution of concentrations of PFT, SO_2 and sulfate attributable to MPP	Vimont (1997)
RAPTAD/ HOTMAC/ ROME	Three-dimensional Lagrangian random puff model; primitive equation meteorological model; Lagrangian plume model with explicit reaction chemistry for gaseous and aqueous conversion of SO_2 and other species	Meteorological soundings, topography and land use, solar radiation; MPP emissions of PFT, SO_2, NO_x, and trace metals; background chemical concentrations; PFT concentrations at receptors	Complete meteorological field; distribution of concentrations of PFT, SO_2 and sulfate in MPP plume, at surface and aloft	Yamada (1997, 1999); Lu and Yamada (1998); Seigneur *et al.* (1997); Karamchandani, *et al.*, (1998);

Table 8-3 Principal Assumptions of the Apportionment Methods

Method	Emissions	Meteorology	Ambient AQ	Sulfur Chemistry	Deposition
RECEPTOR DATA ANALYSES					
Tracer Scaling (Tracer Max)	Constant ratio of MPP SO_2 to PFT emissions	N/A	N/A	100% conversion of SO_2 to particulate S, but not greater than measured value	No deposition
Tracer Regression	Halocarbon represents So. Calif. Source region and mixing ratio represent source region to south; all source regions accounted for by PFT, halocarbon and mixing ratio	N/A	N/A	N/A	No deposition
TAGIT	MPP is only cause for elevated S at tracer-impacted sites	N/A	Background particulate S spatially uniform	N/A	N/A
Modified CMB (MCMB)	Constant ratio of SO_2 plus particulate sulfur to marker species in emissions from all sources except MPP; incoming air mass composition represents profiles for other sources than MPP; halocarbon marks So. Calif. source region	Time of travel deduced from modeled wind field	None	Linear conversion; conversion rate for MPP emissions lower than regional rate; conversion rate for Las Vegas emissions higher than regional rate.	Linear; different rates for SO_2 and sulfate
TMBR	Constant ratio of MPP SO_2 emissions to PFT emissions	N/A	N/A	N/A	N/A
DMBR	Hourly emissions for SO_2 and PFT	Time of travel deduced from modeled wind field; index of cloud cover estimated from photographs	MPP emissions explain some of the observed variability in receptor SO_2	Linear conversion, with rate dependent on cloud cover index; rate "optimized" for best fit with SO_2 measurements	Linear; different rates for SO_2 and sulfate

Method	Emissions	Meteorology	Ambient AQ	Sulfur Chemistry	Deposition
SOURCE EMISSIONS SIMULATIONS					
Modified HAZEPUFF	None	$1/r^2$ interpolation of 3 wind profilers	None	Linear conversion rate based on solar radiation; aqueous conversion assumed to take place when RH > 80% at additional rate of 2%/hr	No deposition
CALMET/ CALPUFF	None	For Meadview impacts, wind field generally derived from MPP profiler sounding using 5-km grid CALMET diagnostic model; for regional impacts used 3 Project MOHAVE profiles with terrain blocking in model; calendar solar radiation, modified by cloud cover; modified PGT diffusion	Measured surface O_3 representative of conditions aloft	Conversion rate based on measured O_3 and RH; daytime "dry" conversion rate set at 2%/hr, "wet" daytime rate at 20%/hr for 3 hours per day, and nocturnal conversion rate at 0.2 %/hr,	Based on micrometeoro-logical parameter estimates for dry deposition and on measured rainfall for wet deposition
RAPTAD/ HOTMAC	None	Wind, temperature, humidity, and clouds derived by 4-km grid HOTMAC prognostic model nudged by data from 3 soundings and 3 radar wind profilers	N/A	None; modeled inert PFT tracer only	None
ROME	None	Used HOTMAC 4-km grid wind field	Assumed background chemical concentrations	Explicit chemical mechanisms for both gas phase and aqueous pahse	Linear; different rates for day and night, vary with species.

N/A = parameter or calculation not applicable for this method
None = No significant assumptions were made

8.3.1 Tracer Max (Tracer Scaling)

The ambient PFT data, scaled by the tracer/SO_2 stack emission ratio, were used to deduce the maximum possible MPP contribution to particulate sulfur at Meadview and Hopi Point if all SO_2 were to be converted to particulate sulfur and there were no deposition losses (Green and Tombach, 1999). Whenever the maximum possible particulate sulfur that was calculated in this way exceeded the measured value, then the measured value was set as the maximum possible value (i.e., it was assumed that MPP contributed 100% of the measured particulate sulfate concentration).

Key assumptions of the Tracer Max method included the following: (1) The ocPDCH tracer and MPP sulfur (emitted as SO_2) were transported and dispersed identically together to the receptor; (2) There was no deposition of tracer or either MPP SO_2 or particulate sulfur enroute; and (3) The tracer/SO_2 emission ratio was constant (i.e., the PFT emissions rate tracked the variations in the SO_2 emissions rate). In actuality, SO_2 and sulfate will undergo some deposition enroute, while the tracer is essentially non-depositing; therefore the ratio of sulfur to PFT decreases in time. The assumption of a constant ratio means that more particulate sulfur is apportioned to the source than is correct.

The fundamental assumption of the Tracer Max tracer scaling approach is that all of the SO_2 is assumed to convert to particulate sulfate or at least enough of it is converted to match the sulfate concentration measured at the receptor. This assumption produces an upper-bound impact of the MPP source -- it is impossible to have a higher contribution. A lower contribution is certainly possible and is likely, especially in the cloud-free conditions under which sulfate formation proceeds slowly.

The confidence in the validity of these upper bound estimates of MPP sulfur contributions is high. It needs to be re-emphasized, however, that the Tracer Max estimates do not indicate what a realistic contribution might be.

8.3.2 Exploratory Data Analyses

Statistical, temporal, and spatial relationships between the ambient concentrations of the PFT released from MPP, SO_2, and particulate sulfur, and of light scattering, measured during the summer intensive were analyzed by Mirabella (1997). This analysis provided qualitative insight into the contributions of MPP to SO_2 and particulate sulfur in various regions and compared the behaviors of these four variables.

Specifically, Mirabella (1997) compared the 24-hour average MPP tracer, sulfur dioxide, and particulate sulfur concentrations across the network and analyzed the spatial and temporal correspondence between these three parameters in addition to light scattering at various individual sites. In addition, the authors examined the correspondence between MPP tracer and light scattering at Meadview for 12-hour and 1-hour averaging time periods. Using a previously-developed meteorological classification scheme (Farber et al., 1997), Mirabella (1997) also evaluated whether their conclusions differed under various meteorological regimes.

8.3.3 Tracer Regression.

The tracer regression method (White *et al.*, 1999) attempts to explain light extinction at Meadview based on contributions from three sources – MPP, Southern California, and southern Arizona/northern Mexico. The light extinction is related to these source contributions through multiple linear regression, in which assumed markers for each of the three sources are the independent variables and b_{ext} at Meadview is the dependent variable. Methylchloroform (an industrial solvent) is taken to represent urbanized Southern California, the mixing ratio of water vapor to air is taken to represent the contribution of air from more humid regions to the south, and the PFT to represent MPP emissions. In each case, the tracer is assumed to be a conservative indicator, as required by the receptor-oriented regression procedure

The principal assumptions of the tracer regression method have to do with the source regions represented by each tracer. Except for the use of PFT as an MPP indicator, these assumptions involve approximation. It is possible that methylchloroform is emitted from industries in other locations besides Southern California. Moist air does not come only from the south of Meadview, although that locale is probably the predominant source region in the summer period for which the method was applied. In either case, if the tracer is not unique to the region or source to which it is assigned, then emissions will be attributed erroneously to that region or source.

It should also be noted that any regression analysis of this kind will underestimate attribution if the "signal" is noisy, as would be the case if the light extinction were to vary because of unaccounted for background effects. (This limitation also applies to other regression based methods such as TMBR below).

8.3.4 TAGIT

The Tracer-Aerosol Gradient Interpretive Technique (TAGIT) (Kuhns *et al.*, 1999) uses PFT data to identify sites which are not significantly impacted by MPP during specific sampling periods and can be considered to represent the regional background concentration. The MPP-attributable particulate sulfur at a receptor is calculated as the measured excess concentration of sulfur over that at nearby sites with background levels of tracer. Sites with tracer levels below 3 sigma of the background concentration were considered to be representative of regional background sulfur concentrations.

The accuracy of TAGIT depends on the assumption that the only cause for increased sulfur above the regional background at locations where PFT is found is emissions from MPP. Under certain conditions, such as when another source is along a trajectory that intercepts the MPP, it is possible that this assumption will be violated, but there is no way to quantify when this occurs. Under those conditions TAGIT will erroneously apportion to MPP the sulfur from the non-MPP source. Because the difference in sulfur particle concentrations in PFT impacted and unimpacted areas is sometimes small, it is possible for TAGIT to attribute a negative concentration impact to MPP. The precision of the TAGIT attribution can be estimated when there are several nearby sites reporting background tracer concentrations near the impacted receptor. For many instances, the variability of these multiple estimates were larger than the particulate sulfur attributed to

MPP by TAGIT. While individual attibutions by TAGIT are noisy, the method is likely to provide credible results of average attribution over the study period.

8.3.5 Modified CMB (MCMB)

The CMB technique involves correlation of the composition of the aerosol at receptors with "profiles" of the composition of emissions from various classes of sources. The product of the analysis is an apportionment of the receptor SO_x (the sum of SO_2 and particulate sulfate) to the selected classes of sources. In its basic form the technique is only usable for conserved species, i.e., ones that do not undergo chemical conversion.

The basic BYU CMB method that was used initially, as described in Section 8.2, was modified into a hybrid technique that includes a representation of chemical conversion of SO_2 to sulfate particles (Eatough, *et al.*, 1999). Slightly different variants of the technique were used for the summer and winter intensive periods. We focus here on the approach that was used for apportionment of sulfur oxides and sulfate at Meadview and Hopi Point during the summer intensive.

The Modified CMB (MCMB) method uses several elemental and chemical tracers of opportunity as marker species for MPP and major source regions (the Las Vegas area, urban Southern California, the San Joaquin Valley, Baja California, southern Arizona and northern Mexico). The source profile for each source region was determined by measuring the elemental and chemical composition of ambient aerosol approaching the study area from the direction of the source of interest. The chemical conversion of SO_2 to sulfate is addressed using reactivities derived from the ROME modeling (see below) and from optimization of assumed linear conversion rates. The transport routes and times of travel are defined by several wind field models and the potential for clouds to affect the chemistry during the transport of MPP emissions is addressed through the Cloud Interaction Potential (CIP) of the DMBR model (see below). It is important to note that the PFT concentration data were used in the evaluation and modification of the model, but are not used as input data.

Fundamental assumptions of the MCMB method are the equal conservation of the tracer and target species and that all significant contributors to SO_2 and sulfate at Meadview and Hopi Point are identified in the CMB profiles. A further assumption in the MCMB approach is that the ratio of SO_x (sum of SO_2 and sulfate) to the marker species in the source profiles is constant from day to day. Profiles and the profile uncertainty for regional sources, such as Southern California, were developed from ambient measurements at substantial downwind distances during a few days. If the ratios vary outside the determined uncertainty or represent mixes of materials from different source regions the method will apportion SO_2 and sulfate incorrectly among sources. Furthermore, regional profiles tend to be more collinear and less orthogonal than profiles for discrete source types.

The MCMB application also assumes that SO_2-to-sulfate conversion rates at any given time are the same throughout the modeling domain for emissions from all sources except Las Vegas and MPP. Las Vegas and MPP conversion rates can be higher and lower, respectively than the conversion rates from other sources. Results of the ROME model calculations were used to parameterize the relative reactivities of emission from MPP and Las Vegas as compared to other

sources. Sensitivity tests have shown that the apportionment of sulfate to sources is sensitive to the relative values that are used.

The MCMB analysis was not able to apportion all of the sulfur oxide present at Meadview for some samples. It was assumed the underattribution of sulfur oxide was due to separation of particles and gases in the nighttime stable MPP plume and the unattributed SO_2 was therefore assumed to have originated from MPP.

8.3.6 TMBR

Tracer Mass Balance Regression (Malm *et al*., 1989; Ames and Malm, 1999) compares the covariance of SO_2 or particulate sulfur measurements with those of the PFT through an ordinary least-squares regression. The regression coefficients are interpreted as indicators of the attribution of the sulfur constituent to MPP.

The merit of the TMBR is the significance of the regression coefficient (P=.03) which allows us to state that there is a highly significant statistical relationship between PFT concentration and ambient sulfate concentration at Meadview. That only a small fraction of the ambient SO_4 variability is explained by PFT ($r^2 = 0.06$) is not surprising, and TMBR neither makes nor does it rely on any assumptions about what this covariability should be. A low correlation coefficient is not counterintuitive given the non-linearity of secondary sulfate production.

8.3.7 DMBR

Differential Mass Balance Regression (Latimer *et al*., 1989, Ames and Malm, 1999) expands on the TMBR approach by explicitly considering the conversion of SO_2 to particulate sulfur. In this hybrid approach, information about transport time from source to receptor and cloud cover is used with linear conversion and deposition rates to estimate the particulate sulfur concentration at the receptor. The rate constants for the conversion of SO_2 and for SO_2 deposition were chosen by statistical optimization of the correlation between the predicted MPP contribution to SO_2 at Meadview and the measured SO_2. This optimization procedure makes no *a priori* assumption about the amount of variability explained by the MPP contribution to ambient SO_2.

In addition to the usual constraint on equivalent behavior of tracer and sulfur emissions, the DMBR method estimates the amount of conversion of SO_2 to particulate sulfur based on a linear conversion rate. The time of travel is estimated from a wind field model and an hourly conversion rate was derived empirically based on a Cloud Interaction Potential (CIP) and the measured concentrations of SO_2. The CIP, derived from observations of clouds in photographs, attempts to reflect the presence of cloud water in the conversion process. But, since the height of the clouds cannot be readily deduced from the photographs, the CIP is a crude indicator of the effect of cloud water on chemical reactions at the MPP plume height.

8.3.8 Modified HAZEPUFF

HAZEPUFF (Latimer, 1993) is a puff model that simulates the transport, diffusion, and deposition of puffs emitted hourly from a source. The puffs are advected by an externally prescribed wind field and diffuse at rates based on the common Pasquill-Gifford stability classes.

Conversion of SO_2 to sulfate takes place linearly in dry air at rates computed by the model based on solar radiation. Whenever the ambient relative humidity is above 80% it is assumed that clouds are present and an additional aqueous conversion rate of 2%/hr is added to the dry rate. Dry deposition is treated linearly with deposition velocities of 0.91 and 0.14 cm/s for SO_2 and sulfate, respectively. HAZEPUFF does not consider wet deposition.

Since HAZEPUFF had limited skill in predicting MPP impacts during the initial model evaluation (See Section 8.2), it was modified for the final attribution assessment. The principal change was an adjustment in stability classes, which reduced the tendency of the model to overestimate concentrations. Also, the puff cross sections were made Gaussian, which is more realistic than the "top-hat" profiles used initially. The wind field used was derived from the three Project MOHAVE wind profilers. These changes improved the performance of the model, when tested against the PFT measurements, giving a bias of 0.84 and $r^2 = 0.24$ at Meadview for 24-hr averages of the PFT concentrations. The correlations for 12- and 1-hr averages were lower than the 24-hr correlations.

8.3.9 CALMET/CALPUFF

CALMET/CALPUFF is a combination of a diagnostic meteorological model (CALMET) and a Lagrangian puff air quality model (CALPUFF). Hourly radar profiler wind data taken during the summer intensive period provide the input data for CALMET. This modeling system was applied only after the PFT data had been made available, and the PFT information was used for making the choice of input wind data.

The CALPUFF/CALMET system was used to simulate two types of conditions, both of which may be considered as bounds to the range in which actual impacts of MPP might lie. One type of conditions, which was simulated for most of the 1992 calendar year (see Section 9.6), is based on the assumption that all sulfate formation took place in cloud-free air. This can be considered to produce a lower bound to the extend of actual sulfate formation. The other type of conditions, which was simulated only for the summer, is based on the assumption that the MPP plume interacted with clouds for a specified period of time each day. Because clouds were not present every day and the assumed period of interaction was long, this condition was taken to approximate an upper bound to potential MPP impacts.

For the first type of conditions, the internal chemistry algorithm of the model was used to calculate the conversion of SO_2 to sulfate. This algorithm is based on homogeneous, "dry" chemistry. For the second type of conditions, where the Mohave Power Plant plume interacts with clouds, aqueous phase chemistry is likely to occur, which would result in much higher conversion rates than the internal algorithm of the model would predict. Therefore, as a bounding exercise, for the the second analysis it was assumed that all the plume material interacted with clouds for three hours every day and the SO_2 was converted to particulate sulfate at a rate of 20% per hour during those three hours. These two analyses, labeled "CALPUFF Dry" and "CALPUFF Wet," respectively, can be considered as estimates of lower and upper bounds to the impacts of MPP emissions

The initial settings and choices of input meteorological data were selected to improve comparisons between predicted and measured PFT concentrations (Vimont, 1997). The wind

fields generated by the CALMET diagnostic meteorological model were derived from three Project MOHAVE radar profilers. The final calculations, which were done for most of the year, were made using only the MPP profiler because it was the only one that operated for nine months. The ability of CALPUFF to predict PFT tracer concentrations was degraded slightly when only the MPP profiler was used for input data. The grid scale of the wind field was 5 km, which is sufficient to represent major topographic features but will smooth over many smaller ridges, peaks, and valleys. The Pasquill-Gifford-Turner (PGT) diffusion algorithm, with transitioning to time-dependent dispersion curves at longer distances, was used to represent the plume diffusion.

CALPUFF simulates daytime SO_2 conversion to particulate sulfur using a linear mechanism with a conversion rate that is based on solar radiation, PGT class, ambient ozone concentration, and relative humidity. The algorithm produces a maximum conversion rate of about 4%/hr at 100% RH, which is lower than generally-accepted peak aqueous conversion rates. On the other hand, the algorithm does not attempt to quantify the time spent in clouds, which could produce a lower hourly-average rate than the peak that occurs whenever the plume is in a cloud. Both of these factors were addressed in the "CALPUFF Wet" upper-bound aqueous conversion calculations by selection of a 20%/hr conversion rate for three hours per day in clouds.

The CALMET/CALPUFF system, with SO_2 conversion turned off, was tested against the PFT data. Two different comparison tests were performed. In the first test, the concentration predicted to occur at the receptor located at the coordinates of the monitor, or at one of the 8 adjacent receptors, was compared with the PFT measurement. The one value of these 9 that best matched each measurement was used in a statistical evaluation of model performance. This test, therefore, assesses how well the measurement was approximated by the model prediction, even though meteorological uncertainty may have cause the prediction to slightly miss the correct receptor location. For Meadview, using only the MPP wind profiler data, the correlation in this best-of-nine comparison was $r^2 = 0.47$. The correlations were even higher at Las Vegas Wash (LVWA; $r^2 = 0.81$) and Dolan Springs (DOSP; $r^2 = 0.80$). These values suggest that the model's transport and diffusion mechanisms are fundamentally sound.

As one might expect, the prediction at the exact receptor cell correlated less well with the PFT measurement there. These correlations were $r^2 = 0.00$ at Meadview and Las Vegas Wash and $r^2 = 0.08$ at Dolan Springs. Such values are similar to those tabulated in Table 8-1 and indicate that the CALMET/CALPUFF system was no better at predicting impact at a specific point than were the methods evaluated initially. Since the CALMET/CALPUFF calculations did not explicitly use the PFT data, such a conclusion is not surprising.

Nevertheless, because of its credible performance in the best-of-nine cell comparison and its computational efficiency, the CALMET/CALPUFF modeling system was used to develop a general estimate of the magnitudes of impacts that might be expected under specific conditions. The conditions chosen were the bounding conditions of, first, a totally cloud-free atmosphere and, second, one with an arbitrary degree of in-cloud conversion. Neither the CALPUFF Dry nor CALPUFF Wet simulation should be considered a realistic representation of impacts under the varying meteorological conditions that actually occur.

8.3.10 HOTMAC/RAPTAD/ROME

The most explicit simulations of the project involved three atmospheric models applied for the period August 6 through 16, 1992. The three-dimensional mesoscale prognostic meteorological model HOTMAC was used for simulating airflows. The three-dimensional Lagrangian transport and diffusion model RAPTAD was used for simulations of transport and diffusion of an inert species (e.g., tracer gas). The result was a 3-dimensional field of winds, turbulence, temperature, and clouds with a horizontal resolution of 4 km. The ROME reactive plume model was then used to simulate chemical reactions and particle formation in the plume.

The turbulence parameterization in HOTMAC is treated in a more rigorous manner than the PGT classification used in CALMET. The combination of HOTMAC and RAPTAD is designated as an "alternative guideline model" in Appendix B of the U.S. EPA's Guideline on Air Quality Models. The application of HOTMAC and RAPTAD here is described in Yamada (1999).

Rawinsonde data on wind, potential temperature, and water vapor mixing ratio at Cottonwood Cove, Dolan Springs, and Page, and radar wind profiler data from Mohave Power Plant, Truxton, and Meadview were used to provide initial and boundary conditions to HOTMAC simulations. The HOTMAC meteorological predictions above 374 m AGL were also "nudged" by these measurements.

RAPTAD used the wind and turbulence distributions modeled by HOTMAC and simulated ocPDCH tracer concentrations from MPP at sampling sites in the study area. Also, hypothetical releases from Reid Gardner Power Plant and the Las Vegas area were simulated.

The RAPTAD-modeled tracer concentrations were compared with the 12-hour or 24- hour averaged concentrations measured at sampling sites in the study area. The overall performance of the model over 8 sites for 11 days gave a bias of 1.54 (i.e. the model values averaged 1.54 times the measurements) and $r^2 = 0.61$. The best performance occurred at Dolan Springs ($r^2 = 0.93$) and Kingman, ($r^2 = 0.83$), based on 11 data points for each. At Meadview alone, however, the 24-hr r^2 was 0.11 and the bias was 2.01, based again on only 11 data points. At Hopi Point, the r^2 was 0.03, with a bias of 0.63.

Using the HOTMAC/RAPTAD plume trajectories and diffusion, the reactive plume model, ROME (Reactive and Optics Model of Emissions) was used to estimate the contribution of the MPP to sulfate concentrations in the Grand Canyon region for portions of the same summer period of August 6 to 16, 1992 (Karamdanchani *et al.*, 1998). ROME uses a Lagrangian approach to describe the transport and dispersion of a plume emitted from a stack, and simulates the gas- and aqueous-phase chemical reactions that occur as the plume mixes with the background air. The model includes state-of-the-science formulations of the governing atmospheric processes as described in Seigneur et al. (1997). The model has been tested for a number of applications similar to the Project MOHAVE exercise (e.g., Seigneur et al., 1999; Gabruk et al., 1997).

Selected HOTMAC/RAPTAD plume trajectories originating at MPP and arriving at Meadview or Hopi Point were simulated, taking the plume height to be the initial value calculated by the model. Measured tracer concentrations at these two locations were used to scale modeled sulfate concentrations attributable to MPP emissions of SO_2. Particulate sulfate measurements at

Meadview and Hopi Point were used to estimate MPP sulfate contribution relative to measured values. Trajectories were selected based on their potential for interaction with clouds, their proximity to the two receptor locations, and their plume dimensions to provide a comprehensive representation of the range of MPP plume settings that impact the two receptors.

Ambient (background) concentrations were inferred from limited surface and aircraft measurements of VOC, CO, ozone, NO_x, H_2O_2, SO_2, NH_3, Fe and Mn concentrations from the Project MOHAVE database. Literature review and consultation with experts were used to obtain background concentrations for species that were not measured, such as formaldehyde, other aldehydes, and PAN.

Plume conditions, including plume trajectory data (location, width, and vertical mixing) and meteorological data (temperature, relative humidity, pressure, and cloud liquid water content) were based on the HOTMAC and RAPTAD output. Emissions of SO_2, NO_x and PFT from MPP and the measured ratios of MPP Fe and Mn emissions to SO_2 emissions were other inputs.

Wherever information needed to conduct the simulations was not available or was available in the form of a range, the conditions chosen were those that would provide an estimate of the largest reasonable MPP contribution to the sulfate concentration at the receptor. In addition, sensitivity studies were conducted by varying several input parameters over their plausible range of values.

Clouds were assumed to exist whenever the estimated cloud water content (from HOTMAC output) was higher than 0.01 g/m^3. All such cases during the 11-day period were simulated. Net updraft velocities in clouds were assumed to be zero.

The MPP puffs were assumed to be non-overlapping to maximize the SO_2 oxidation rates under oxidant limited conditions in the plume. Realistic, but lower than expected dry deposition velocities for SO_2 and sulfate were used. This would contribute to a slight overestimation of atmospheric SO_2 and sulfate concentrations.

8.3.11 Evaluation of Windfields

An important component of the numerical models used to apportion MPP SO_2 and sulfate is the accuracy of the windfields. Koracin *et al*. (1998) developed a method that utilizes tracer measurements to compare and evaluate wind fields as predicted by different atmospheric models or obtained from interpolation and extrapolation of measurements. The technique evaluates only the windfields prior to the incorporation of dispersion calculations. Windfields that transport tracer close to the receptors with high measured tracer concentration score highest using this method. Details of the method are provided in the Koracin *et al.* paper, which is included in Appendix C. The main objective of the method is to quantitatively describe and indicate which wind fields are best able to reproduce the main transport of tracers. The method has been applied to MPP tracer (ocPDCH) measurements conducted in summer 1992. Wind fields obtained from four atmospheric models CALMET (Vimont 1997), HOTMAC (Yamada and Bunker 1988), MM5 (Grell et al. 1995), EK (Enger et al. 1993, Koracin and Enger 1994) were tested. For the limited period in which windfield data were available from all four models (8/6/92 – 8/13/92), the analysis indicated that the performance of the CALMET, EK, and MM5 and wind fields were

comparable, while HOTMAC scored slightly higher for the 10 day it was employed(i.e. was more accurate) than the other models.

8.4 Computer Simulation of Visual Air Quality

In order to assist in interpreting the quantitative data on the MPP impact on the light extinction coefficient, b_{ext}, that was developed using the models described above, various levels of visibility degradation in typical Grand Canyon National Park views have been displayed in images that can be viewed on a computer screen. Two views in GCNP, one at Tuweep, at the western end of the park, and the other at Desert View, located east of Hopi Point, were used for this purpose. In each case, mathematical models of radiative transfer were used to calculate the changes in the appearances of these views due to various levels of light extinction. The approach used to generate these simulated views is described here. The actual views are contained in a CD-ROM that accompanies this report and are described in Section 9.8.

8.4.1 Radiative Transfer Concepts

Radiant energy, as it passes through the atmosphere, is altered by the scattering and absorption by gases and particles. Image-forming information is lost by scattering of radiant energy out of the sight path and absorption within the sight path. Further, ambient light from direct, diffuse, and reflected radiance is scattered into the sight path. This adds radiant energy called "path radiance" to the observed radiation field, so that

$$N_r = N_o T_r + N^* \qquad (8\text{-}1)$$

where:
- N_r = observed image radiance at distance = r
- N_o = inherent image radiance at distance = 0
- T_r = transmittance of sight path of length = r
- N^* = path radiance of sight path

The transmittance of the sight path is calculated from measured extinction or the distribution of particles and gases along the sight path. The path radiance is more difficult to estimate. A reasonable assumption under uniform illumination (cloud free sky or uniform overcast) is to estimate the path radiance with an equilibrium radiance model:

$$N^* = N_s(1 - T_r) \qquad (8\text{-}2)$$

where
- N_s = sky radiance at horizon above sight path

These equations can be applied to each pixel of a photographic image, to represent the effect of the atmosphere on that image.

The bulk atmospheric optical properties such as extinction, scattering, and absorption coefficients, single scattering albedo, and the scattering phase matrix are required to apply the above equations to each element of a scenic view. They are calculated by an aerosol model. The Mie theory model assumes spherical particles for externally-mixed, homogeneous or internally-mixed, coated aerosols.

A backward photon trajectory, multiple scattering, Monte Carlo, radiation-transfer model was used to calculate sky radiances. The inherent radiance of each terrain pixel was estimated with the equilibrium radiance model, sky radiance model, and distance to the target for each pixel.

The modeled image radiance field for a selected level of extinction was then calculated by first using the new extinction value and distance to each terrain pixel to calculate a new path transmittance. Second, the new path radiance was calculated using this transmittance and modeled sky radiance in Equation 8-2. Third, the new apparent image radiance field was calculated by using these values in Equation 8-1. These new image radiance files were then used in the image processing modules to generate the final images, as described below.

8.4.2 Image Processing Techniques

The original images that started the process described above were two 35 mm color slides taken at Tuweep and Desert View. The slides necessarily represent cloudless skies under the cleanest visual air quality conditions possible. Aerosol and optical data associated with the day the picture was taken were also used.

Color film may be regarded as a measurement tool that creates a map of an incident image spectral radiance field. The film's red, green and blue emulsion layers collect the radiation and convert it through chemical changes to exhibit varying density values related to the initial scene element radiances. The time interval that the film views the scene multiplied by the radiance of the scene element is known as the exposure of the film. Since every pixel of a slide is exposed for the same time interval, the varying densities are directly related to the initial scene element radiance (N_r).

The slide image was digitized through three wide band filters at different colors. The typical spectral function results in nearly Gaussian filters with peaks centered near 650 nm (red), 550 nm (green), and 450 nm (blue), with little overlap of the effective filter responses. Each terrain pixel in the image was then assigned a specific distance, elevation angle and azimuth angle with respect to the observer position, using detailed topographic maps of the area.

To produce the new image, which displays the scene appearance at a chosen level of extinction, the above information was used in the calculation of a new radiance field. That modeled radiance field describes the appearance of every pixel on the photograph, each of which has been altered by the scattering and absorption that were artificially added to the initial image. The results, when viewed as a photograph or on a color computer monitor, then portray the original digitized photograph under the different atmospheric conditions. The two views are portrayed under 13 different extinction levels in the CD-ROM enclosed with this report.

8.4.2 Human Perception of Visibility Change

In order to better understand the perception of the changed visibilities in the images on the CD-ROM, it is useful to briefly discuss some aspects of the human perception of visibility changes.

Human perception of changes in visual air quality is a complex function of atmospheric properties such as lighting conditions, cloud cover, and ambient extinction; scene characteristics

such as size, shape, color, texture and distance to features; and observer characteristics. A robust complete model of human perception of visual air quality has yet to be developed. Nevertheless, reasonably valid concepts can be developed from a simple analysis of apparent target contrast:

$$C_r = 1 - \left(\frac{{}_t N_r}{{}_s N_r} \right) \qquad (8\text{-}3)$$

where:

C_r	=	apparent target contrast at distance r
${}_tN_t$	=	background sky radiance at distance r
${}_sN_r$	=	target radiance at distance r

Apparent target contrast can be further defined as:

$$C_r = C_0 \exp(-b_{ext} r) \left(\frac{{}_s N_0}{{}_s N_r} \right) \qquad (8\text{-}4)$$

where:

C_r	=	apparent target contrast at distance r
C_0	=	inherent target contrast at distance r = 0
b_{ext}	=	average extinction coefficient of sight path
r	=	distance to observer
${}_sN_0$	=	sky radiance at target r = 0
${}_sN_r$	=	sky radiance at distance r

Apparent target contrast is a good indicator of visibility. As the extinction goes up, C_r decreases, (i.e. the target becomes less noticeable). As extinction decreases, the target becomes more noticeable (i.e. darker against the background). Apparent target contrast can be used to determine whether the target can be perceived and, when perceived, the apparent contrast can also be used to evaluate the visual quality of its appearance.

With the assumption of equal sky radiances at the target and observer (uniform illumination of the scene), equation 8-4 reduces to:

$$C_r = C_0 \exp(-b_{ext} r) \qquad (8\text{-}5)$$

Equation 8-5 can now be used to determine the change in C_r for various targets as a function of changes in extinction. For example, Figure 8-1 plots the calculated changes in contrast (delta contrast) of targets from 1 to 100 km distant as a function of percent changes in extinction at Grand Canyon National Park during a condition representative of the MOHAVE summer intensive. An inherent contrast of -0.80 was assumed for all targets, which approximates the appearance of a dark scenic element against the horizon sky.

As extinction is decreased, at some level of delta C_r , changes in visual air quality become perceptible. There is uncertainty as to the actual size of delta C_r that is detectable, and the value differs from individual to individual and varies with viewing condition. A value of 2% contrast change (delta C_r = 0.02) is sometimes used as an approximation, and that value is marked on Figure 8-1. With an assumed perceptible threshold of 0.02 in delta C_r and the assumed target

contrast of –0.80, Figure 8-1 indicates that all targets past 15 km distant will experience perceptible changes in apparent contrast (i.e., delta $C_r > 0.02$) with a 10% decrease in the light extinction coefficient. If the target has less contrast or the human perception threshold is larger, then a larger change in extinction will be required to produce a perceptible change. For example, if the contrast change threshold is 0.05 (another values that is sometimes used), then the decrease in light extinction would be imperceptible on Figure 8-1.

The simplified model illustrates some of the general concepts of detection of visibility change. Real scenes have elements of varying contrasts and color at different distances, and so their response to a change in extinction is not easily shown quantitatively. The images on the CD-ROM provide a qualitative representation.

We should note here that the fractional change in extinction is generally considered to he proportional to the human response, e.g.., a 20% change in extinction is perceived similarly whether the change in visibility is from 100 km to 80 km or from 10 km to 8 km. This is the basis for the deciview scale for representing extinction (Pitchford and Malm, 1994).

The simulation of human perception of actual scenes by using photographs or computer images is not perfect, however. Based on color matching experiments performed at the Grand Canyon, Henry (1999) points out that such images are less colorful and more blue than the true scenic view that is observed on site. These conditions appear to derive from the limitations of the photographic film that is the basis for the initial images that were digitized. A consequence of these limitations is that the artificial images overstate the visual effects of increasing haziness.

Consequently, one should not rely on the computer images to provide quantification of thresholds of human perception of visibility change in terms of extinction changes. Rather, these images should be considered approximations that portray the essential effects of extinction change, albeit only semi-quantitatively.

8.5 Discussion of Assessment Results

Each of the assessment methods except Tracer Regression and the exploratory data analysis produced estimates of the MPP-contributed sulfate at Meadview during the summer intensive monitoring period. Several methods also provided results at Hopi Point and/or for the winter intensive monitoring period.

Time plots of the 12-hour estimated MPP-contributed sulfate at Meadview and Hopi Point for all of the assessment methods are shown in Figure 8-2 through Figure 8-7. TAGIT results, which are limited to 24-hour duration estimates, are displayed as double 12-hour points at the same level for each day. Note that TAGIT occasionally produces negative contribution estimates. These occur when the particulate sulfur concentrations at nearby monitoring sites with little or no tracer were, on average, somewhat higher than that at the receptor site. These negative values should be interpreted as zero contribution by MPP.

All methods agree on the relative importances of the four site - season combinations (compare vertical scales), with Meadview having greater impact in either season than Hopi Point and summer showing greater impacts than winter. Meadview summer measured particulate sulfate and a method labeled Tracer Potential are also shown in Figure 8-4. Tracer Potential is Tracer

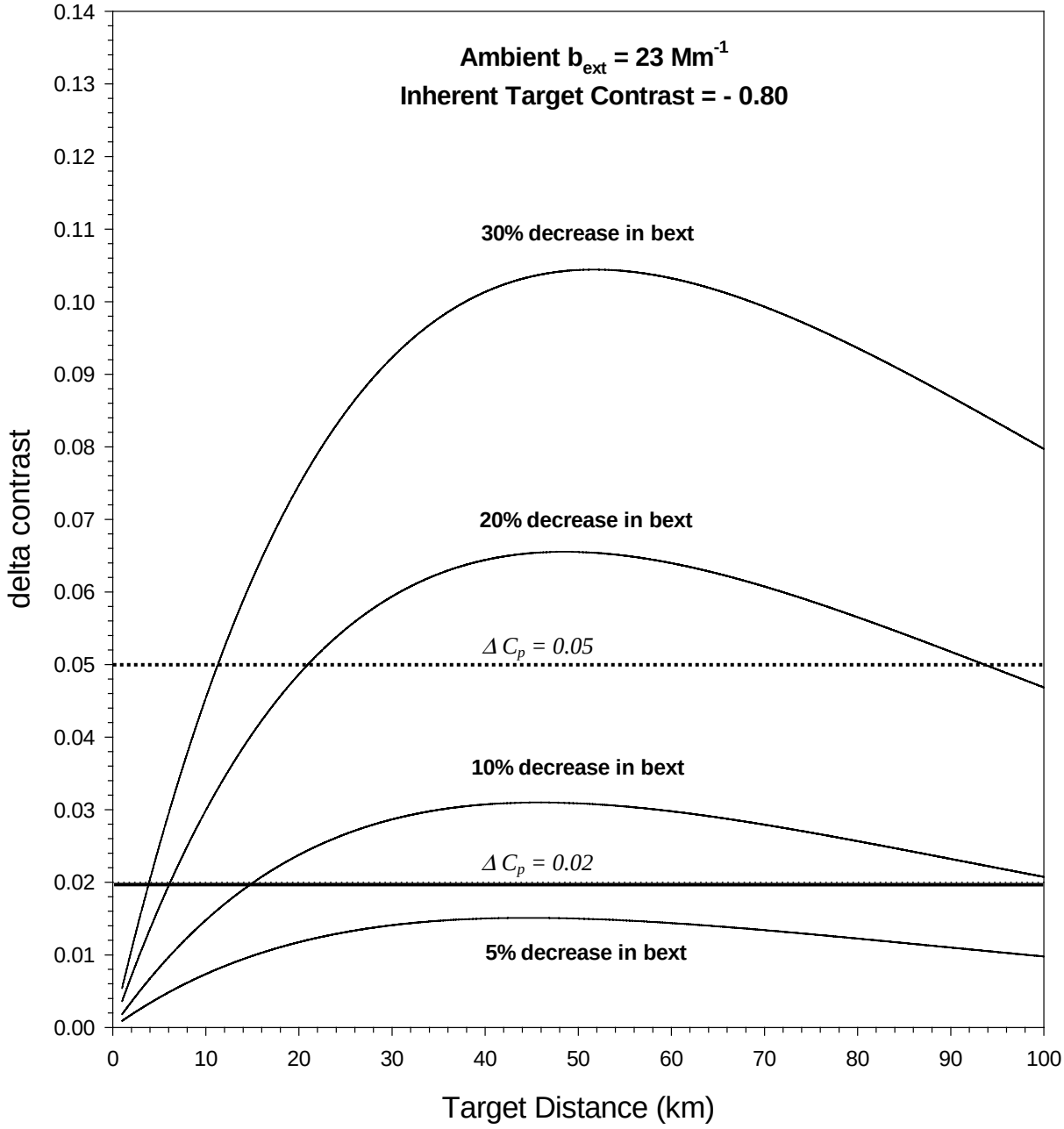

Figure 8-1 Change in apparent target contrast for % change in ambient extinction.

Max without the constraint of substituting the measured sulfate from the tracer scaled SO_2 when the tracer scaled SO_2 exceeds the measured sulfate. Thus, Tracer Max (not plotted) is either equal to measured sulfate or Tracer Potential, whichever is lower. It was included in this plot to show the effects of that constraint, which is important for about half of the summer intensive monitoring periods at Meadview. This was done to show that there are many periods where the tracer data provide a considerably more restrictive upper bound than the measured sulfate.

The Meadview summertime plot is the most useful for the comparison of the various methods' estimates. Many, but not all, methods agree on which time periods have relatively high estimates

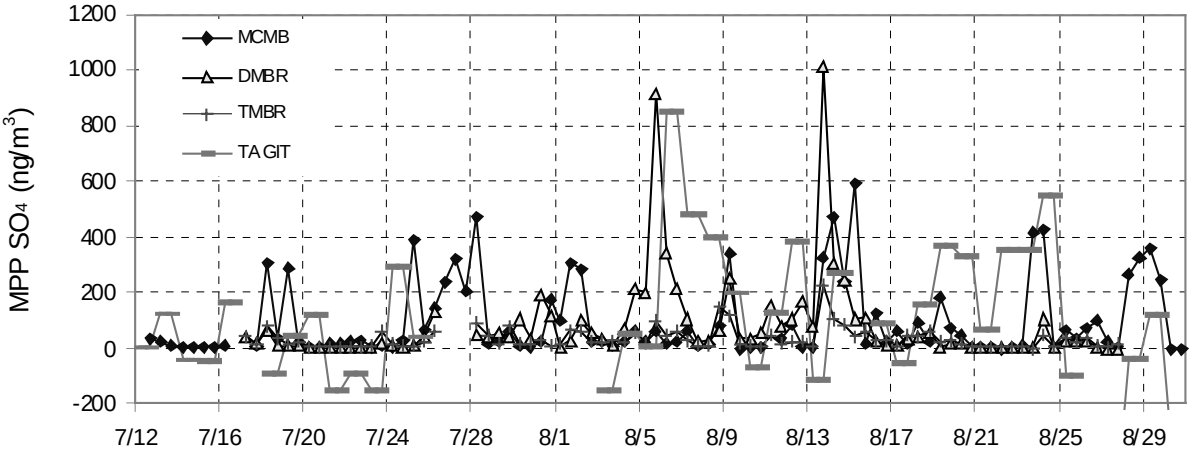

Figure 8-2 Source attribution sulfate time series from receptor models for MPP at Meadview during the summer intensive.

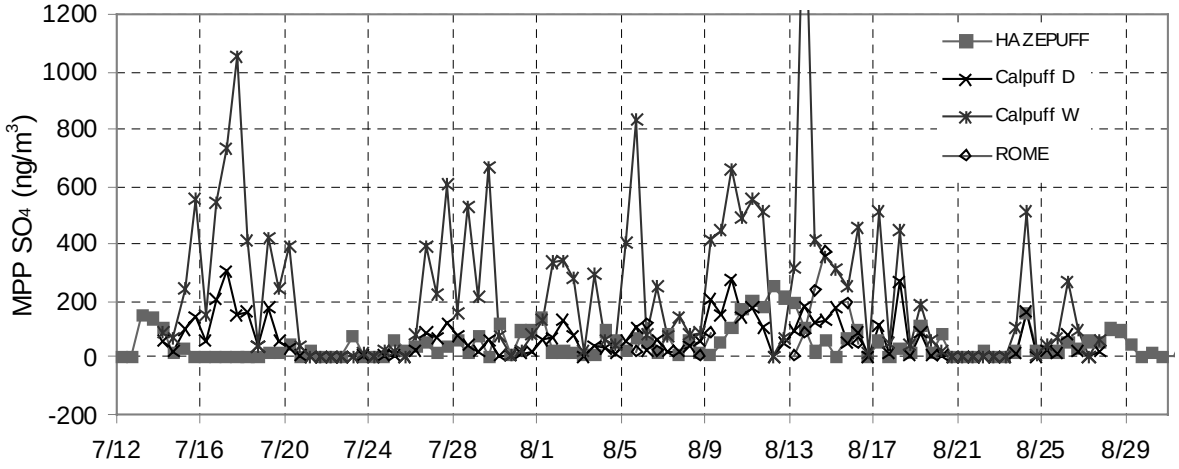

Figure 8-3 Source attribution sulfate time series from simulation models for MPP at Meadview during the summer intensive.

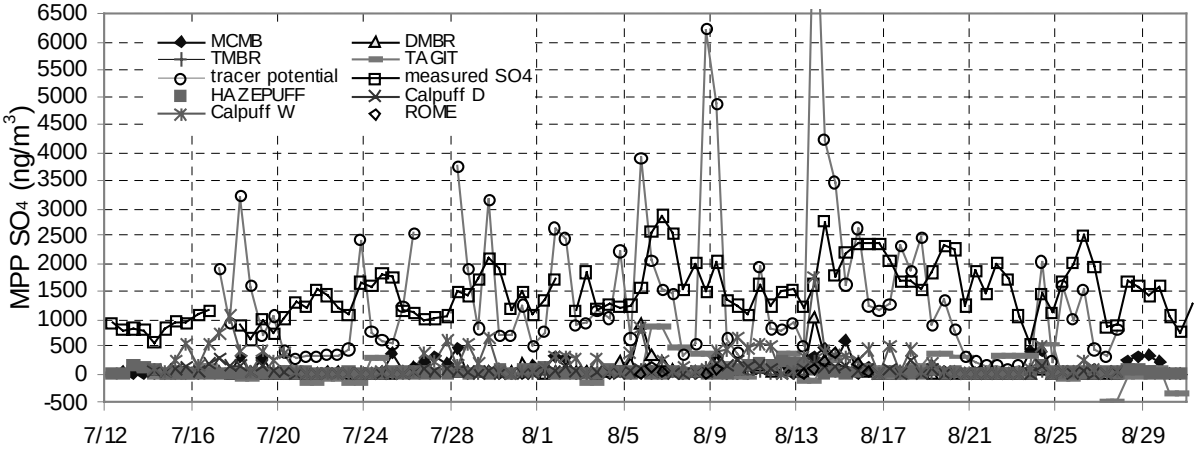

Figure 8-4 Source attribution sulfate time series from all models for MPP at Meadview during the summer intensive. Measured sulfate and tracer potential are also included for comparison.

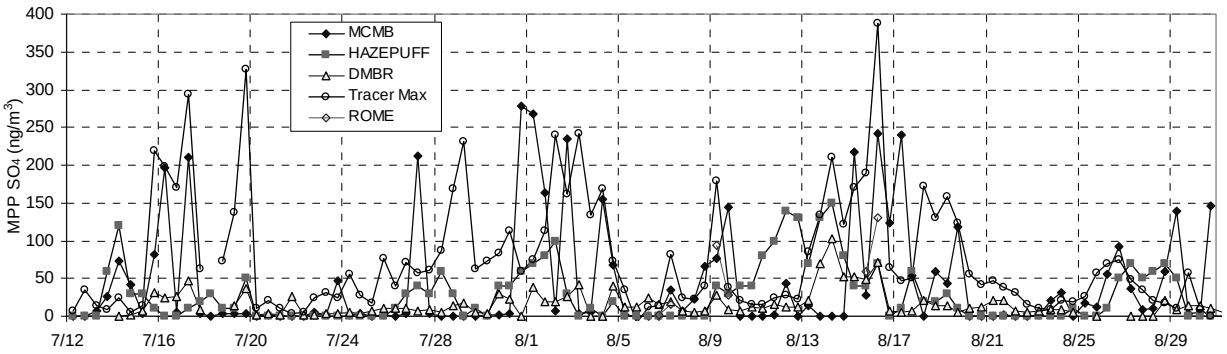

Figure 8-5 Source attribution sulfate time series for MPP at Hopi Point during the summer intensive.

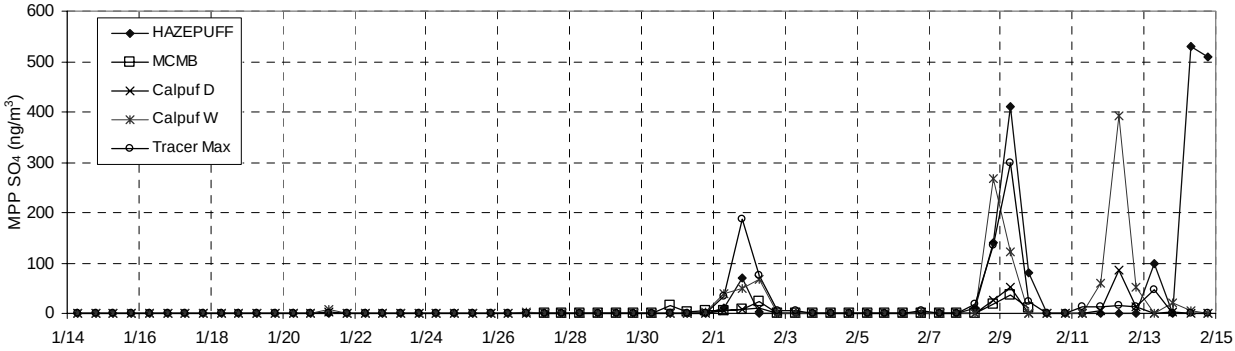

Figure 8-6 Source attribution sulfate time series for MPP at Meadview during the winter intensive.

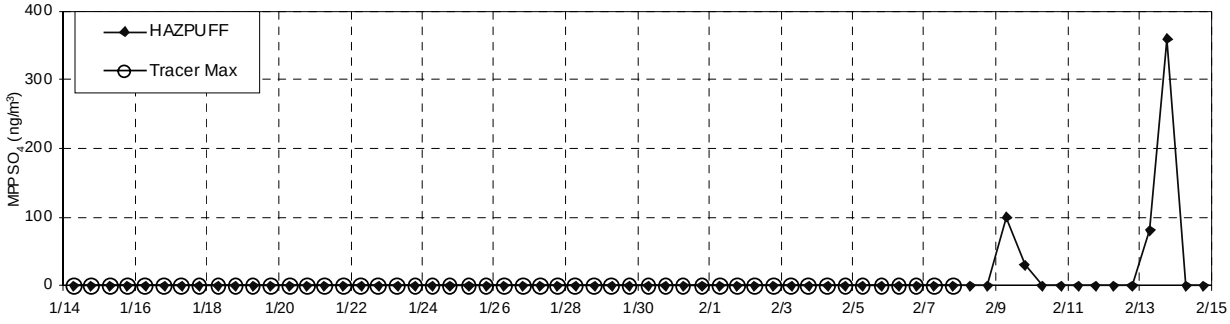

Figure 8-7 Source attribution sulfate time series for MPP at Hopi Point during the winter intensive.

of MPP sulfate contributions. Much of the agreement can be explained as due to the common use of tracer concentration or the skill of some methods to estimate it (all methods except TAGIT and HAZEPUFF). For these methods that tend to agree on high impact periods, only high tracer concentration periods are candidates for high estimated MPP contribution to particulate sulfate. Variations in the peaks among these methods are probably mostly due to differences in the approaches used to represent the process of SO_2 to particulate sulfate conversion. For example, CALPUFF Wet assumes some wet conversion for every time period and so it estimates peaks

from July 15 to July 20 where the other methods, by assumption or by incorporation of data, knew that only dry chemistry occurred on those cloud-free days.

Among the methods that used tracer data, TAGIT is unique in that the PFT concentration was not used to determine the primary emission impact of MPP at the receptor site. It was only used to classify sites as MPP-impacted or background sites, so that the average particulate sulfate concentration at the background sites could be subtracted from the receptor site concentration. TAGIT peaks are not well correlated with tracer peaks or with the peaks of most of the other methods. In fact there are a number of time periods where TAGIT produces very small estimates when the other methods produce peaks and TAGIT peaks when other methods have rather small estimates.

This substantial temporal discrepancy between TAGIT estimates and those of the other methods was the cause of considerable technical debate among the project analysts. For any of the periods with substantial disagreement, if TAGIT is correct then the other methods are incorrect or if the other methods are correct then TAGIT is incorrect. A number of difficult questions were examined. How can MPP contribute a substantial amount of sulfate (estimated by non-TAGIT methods), if the concentrations of sulfate outside of the MPP impact area are as high as inside the impact area (TAGIT)? Can the higher sulfate concentrations at a receptor site compared to those at a tracer-free background site be just a coincidence and not imply an MPP contribution? The conclusions from these discussions are that both the TAGIT and non-TAGIT methods can be incorrect for any specific time period. TAGIT can be fooled by background gradients caused by pollution fronts as they traverse the region. The non-TAGIT approaches require information about the oxidation of SO_2 to particulate sulfate and the rate of SO_x deposition. Small errors in these representations can have a major effect on the sulfate concentration predictions.

Unfortunately, for the periods of disagreement, no procedure was discovered to determine which of the methods is more likely to be incorrect. TAGIT is unique among the methods in not requiring the highly uncertain use of some approach to account for SO_2 conversion. Had estimates from TAGIT agreed fairly well with those from any of the other methods on a day-by-day basis it would have strengthened the confidence in those results substantially. However, this is not the case.

Decisions on managing MPP emissions will likely turn on the frequency distribution of MPP's sulfur contributions rather than its contributions to any specific sampling period. In section 9.4 the results from the various methods are accordingly displayed as cumulative frequency distributions. Some project analysts are uncomfortable with this form of presentation, however. The principal concerns are that (i) the format conceals the lack of agreement between models evident in the time series in Figure 8-2, Figure 8-3, and Figure 8-5, and (ii) the inclusion of bounding estimates (from Tracer Max and CALPUFF Wet and Dry) in a percentile plot invites misinterpretation. These concerns are discussed in the following paragraphs.

The lack of agreement among models as to when MPP impacts were most likely to have occurred undercuts our confidence that any of the models reliably represent the essential atmospheric processes involved. The cumulative frequency plots in section 9.4 appear to show better agreement between the various models; in particular, all of the non-bounding estimates

yield similarly small impacts during at least 50% of the sampling periods. The viewer of these plots must bear in mind, however, that the sampling periods contributing to the upper percentiles of one model may be those contributing to the lower percentiles of another. Consequently, the conclusions about relative MPP contributions drawn from the frequency distributions must be deemed to be less rigorous than those conclusions that are derived directly from the model outputs.

In particular, it should be recognized that every point in the cumulative frequency distributions for bounding estimates (CALPUFF Dry at the lower bound and CALPUFF Wet and Tracer Max as upper bounds) meets specific bounding assumptions. Therefore, such bounding distributions do not approximate any real distribution in which conditions range from those at the lower bound to those at an upper bound. Furthermore, it cannot be assumed that actual dry conditions are represented by the lower percentile values of CALPUFF Dry and cloudy conditions are bounded by the upper percentile values of CALPUFF Wet. Depending on the extent of ventilation during dry and wet conditions, it could very well be that cloudy conditions are bounded by the lower percentile values of CALPUFF Wet, or by a selection of points from throughout the distribution. Also, for example, if a 90^{th} percentile CALPUFF Wet concentration corresponds to an actual condition, that condition may be at the 97^{th} percentile (or, conversely, at the 85^{th} percentile) in the actual distribution resulting from both dry and wet conditions

The reality is that we don't know the frequency of cloud interaction, nor do we trust that any of the models consistently provides the true impact under dry or wet chemistry conditions. The result is that we are unable to indicate the amount of distortion in what are in fact only estimates of bounding curves. However, the bounding estimates are displayed in the next section despite these problems because some of the analysts thought it useful to identify the bounds of a range of results that is likely to include the true distribution of MPP contributions.

The only truly indisputable bounds are zero impact for a lower bound and the Tracer Max curve for an upper bound. However, these represent highly unlikely conditions of 0% and 100% conversion of MPPs SO_2 to particulate sulfate (or for some periods Tracer Max is 100% of the measured sulfate, which is also highly unlikely). Though the range of results between these two bounding conditions is certain to include the true distribution, it is unrealistically large and is not recommended as the basis for judging the range of MPP impacts.